Available online at www.sciencedirect.com
ScienceDirect
Journal of Non-Crystalline Solids 352 (2006) 5164–5169
JOURNAL OF NON-CRYSTALLINE SOLIDS
www.elsevier.com/locate/jnoncrysol

Local dimensionality and intermediate range ordering of ion conduction pathways in borate glasses

Andreas Hall [a,*], Stefan Adams [b], Jan Swenson [a]

[a] Department of Applied Physics, Chalmers University of Technology, S-412 96 Göteborg, Sweden
[b] Department of Materials Science and Engineering, National University of Singapore, Singapore 117576, Singapore

Abstract

Conduction pathways in metal halide doped silver, lithium and sodium diborate glasses have been examined by bond valence analysis of Reverse Monte Carlo (RMC) produced structural models of the glasses. Although all glass compositions have basically the same short-range structure of the boron–oxygen network it is evident that the intermediate-range structure is strongly dependent on the type of mobile ion. The differences are particularly large for the highly doped glasses, where the AgI salt is homogenously introduced to the glass causing an expansion of the B–O network with the formation of pronounced conduction pathways between neighboring borate segments. In contrast, the dopant salts LiCl and NaCl are considerably more inhomogeneously introduced forming microscopic clusters of salt ions, but also regions containing almost no salt ions. The network of the conduction pathways is directly related to the real (atomic) structure, and therefore reflects its features. The characterization of the conduction pathways is discussed in relation to the experimentally observed ionic conductivity.

PACS: 61.43.Fs; 66.10.Ed; 61.43.Bn

Keywords: Diffusion and transport; Glasses; Modeling and simulation; Monte Carlo simulations; Borates

1. Introduction

A fundamental understanding of the microscopic ion conduction mechanism in glasses is a longstanding problem [1]. While ion sites in crystalline materials are mostly well defined and the conduction process can be described in a natural way as a hopping process among these sites, the inherent disorder of the glassy state renders an exact description of sites for ions impossible. All ions differ slightly in their local environments. Experimentally determined atomic pair correlation functions, $G(r)$, are able to describe the average coordination of the mobile ion, but fail to provide any insight into the mechanism of ionic motion from one site to another one. Moreover, it does not give us any hint about the nature of the conduction pathways, e.g., whether a moving ion has a large number of target sites to choose between (and therefore is able to migrate basically everywhere in structure) or is restricted to find one of a few number of available sites in a thin low-dimensional conduction pathway. This latter issue can be elucidated using the concept of bond valence which produces plausible mobile ion pathways in static glass models constructed by e.g. Reverse Monte Carlo (RMC) modeling [2,3]. Although these conduction pathways are not forming a true fractal structure, the concept of fractal dimension of mass [4] can be used to determine their local dimensionality. Moreover, the concept of pair correlation function, commonly used to describe the local structure of liquids and amorphous solids as discussed above, can be applied to describe the correlation between volume elements in the conduction pathways. In this way the intermediate-range structure of the pathway network can be

* Corresponding author. Tel.: +46 7725175.
E-mail address: andreash@fy.chalmers.se (A. Hall).

0022-3093/$ - see front matter © 2006 Elsevier B.V. All rights reserved.
doi:10.1016/j.jnoncrysol.2006.01.166

elucidated and compared with the atomic structure of the glass.

In this paper we have used the concepts of fractal theory and pair correlation functions to perform a detailed statistical analysis of the conduction pathways in Li-, Na- and Ag-conducting borate glasses. We describe the methods and compare the obtained structure of the pathway network with the atomic structure of each glass.

2. Previous structural findings on ion conducting borate glasses

In the case of borate glasses NMR [5–8], Raman [9,10] and infrared experiments [11] have shown that the number of three-coordinated borons, typical of pure B_2O_3, decreases while tetrahedral BO_4 units are formed. For the diborate composition M_2O–$2B_2O_3$ approximately 45% of the borons are four-coordinated. The introduced cations are coordinating to the negatively charged BO_4 units and their effect on the intermediate-range structure of the glass depends on their size and degree of covalency [12]. However, the structural differences between different undoped diborate glasses are in general relatively small [12–14].

Let us now turn to the salt doped borate glasses where diffraction experiments [13,14] and spectroscopic techniques [5,15] have shown that the dopant ions are introduced into the glass structure without seriously affecting the local structure of the boron–oxygen network. In these glasses almost all cations coordinate to both oxygens and halide ions, at least in the case of the highly doped glasses [13,14,16,17]. There are no evidences for substantial differences in the short-range structure (<5 Å) between different metal-halide doped glasses [13,14]. However, on an intermediate-range length-scale of 5–20 Å there are considerable differences between the LiCl, NaCl and AgI doped glasses. Neutron diffraction experiments have indicated a substantial intermediate-range ordering in AgI-doped glasses, which seems to be absent in the LiCl and NaCl doped borate glasses [13,14]. Reverse Monte Carlo (RMC) modeling of the glasses have shown that the intermediate-range order in the AgI doped borate glasses is mainly due to a typical distance of 8–10 Å between neighboring chain-like segments (separated by salt ions) of the boron–oxygen network [13]. No such structural ordering is observed for the LiCl and NaCl doped borate glasses, where RMC modeling indicates that the salt ions are considerably more inhomogeneously distributed than in the AgI doped glasses, forming small salt clusters of widely different shapes and sizes [14]. These salt-rich regions are separated from each other by small boron-rich clusters that retain a similar structure as in the corresponding undoped glass. The inhomogeneties are particularly pronounced for the NaCl doped borate glasses.

To understand how these structural differences between the glasses affect the ionic conductivity it is illustrative to relate the structural findings to the experimentally measured conductivities of the glasses [18,19], summarized in Fig. 1. From this figure it can be seen that the highest conductivities are obtained for the Ag-conducting glasses, while the Na-conducting glasses have the lowest conductivities. However, one should note that the increase in conductivity with increasing dopant concentration is similar for the three glass series, and even slightly larger for the NaCl doped glasses than for the LiCl and AgI doped glasses. Thus, it is not obvious how the structural differences caused by different dopant salts are related to the ionic conductivity.

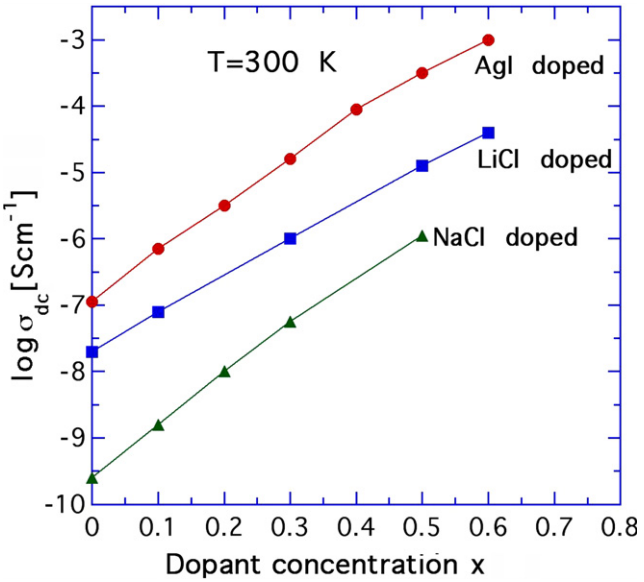

Fig. 1. DC conductivity as a function of salt concentration x for the glasses $(AgI)_x$–$(Ag_2O–2B_2O_3)_{1-x}$, $(LiCl)_x$–$(Li_2O–2B_2O_3)_{1-x}$ and $(NaCl)_x$–$(Na_2O–2B_2O_3)_{1-x}$. The lines are given as guides to the eye. Conductivity data is taken from Refs. [18,19], where no error bars are presented.

3. Computational methods

The experimental procedures and the details of the RMC modeling are extensively described in Refs. [13,14], and will therefore not be repeated here. However, it should be noted that the local environments of the mobile cations in the final RMC configurations of the glasses have been slightly improved since then by the inclusion of a soft bond-valence constraint in the simulations, as described in Ref. [20]. The energetically most favorable conduction pathways in the glasses have been determined by the bond-valence method [21]. It is assumed that the total bond valence sum V of a M^+ ion may be expressed as

$$V = \sum_X s_{M^+-X}, \tag{1}$$

where the individual bond-valences s_{M^+-X} for bonds to all adjacent anions X are commonly given by

$$s_{M^+-X} = \exp\left[\frac{R_0 - R_{M^+-X}}{b}\right]. \tag{2}$$

The bond-valence parameters R_0 and b are deduced from a large number (typically about 100) of crystalline

compounds containing the same M^+–X pairs, but having different coordination numbers and bond-length distributions. In all these different environments and coordination types a monovalent cation should have a bond valence sum close to $V_{\text{ideal}} = 1$. From least squares refinements of R_0 and b we obtained the parameter values given in Table 1 (see also Ref. [22] for a wide range of different $M^+ - X$ pairs). As for the crystalline compounds the ion transport process from one equilibrium site to another should follow the route which requires the lowest valence mismatch $\Delta V = |V - V_{\text{ideal}}|$, corresponding to the energetically most favorable pathway. Thus, in principle the activation energy E_σ should be directly related to ΔV. However, since our structural models are of a relatively small size (about 4000 atoms) and ΔV shows large variations in the structure it is not an easy task to determine the absolutely lowest value corresponding to the experimentally measured E_σ. A better way to quantify E_σ has shown to be to determine the pathway volume for a given value of ΔV [16]. For this purpose the RMC produced structural models were divided into about 4 million cubic volume elements (with a size of ca. $(0.2\ \text{Å})^3$), and ΔV was calculated for a hypothetical mobile ion at each volume element. The volume elements are classified as 'accessible' for a cation if $\Delta V < \Delta_0\sqrt{m_{M^+}}$ or if $V - V_{\text{ideal}}$ changes its sign across the volume element. Δ_0 is a resolution dependent parameter whose exact value is not a critical quantity when comparing the resulting pathways in different glasses to each other, here we have used $\Delta_0 = 0.0266\ \text{amu}^{-1/2}$ (cf. Ref. [16,23]), and m_{M^+} is the mass of the mobile ion. The second criterion is needed to cushion the influence of our limited grid resolution. Accessible volume elements that share common faces or edges belong to the same 'pathway cluster'. If such a pathway cluster percolates through the structural model it is considered to contribute to the dc conductivity.

It is the topology of these percolating pathway clusters we have studied in detail in this work. More exactly, we have performed a statistical evaluation of the percolating pathway clusters (i.e. the conduction pathways) in the ion conducting glasses $(LiCl)_x$ $(Li_2O–2B_2O_3)_{1-x}$ $(x = 0,\ 0.5)$, $(NaCl)_x$ $(Na_2O–2B_2O_3)_{1-x}$ $(x = 0,\ 0.5)$ and $(AgI)_x$ $(Ag_2O–2B_2O_3)_{1-x}$ $(x = 0,\ 0.6)$. In the investigation of the pathways we are using the concepts of fractal dimension and pair correlation functions to classify the network topology. A percolating pathway does not form a true fractal object but due to its irregular structure and local dimensionality, the concept of fractal dimension is a useful tool to investigate its topology. There are several different definitions of fractal dimension [4], here we have restricted ourselves to the concept of mass–radius dimension. For a fractal object F, it is defined by the relation

$$M(r) = c \cdot r^{D_m}, \tag{3}$$

where $M(r)$ is the mass of $F \cap \{x{:}|x - x_0| < r;\ x_0 \in F\}$ (if F is bounded, x_0 is in general chosen as the center of the fractal object, either mass center or geometrical center), c is a constant and D_m is the fractal mass dimension. This dimension may thus be evaluated as the slope of the $\ln(M)$ vs. $\ln(r)$ plot and should, for a natural fractal object, form a straight line over at least a decade. Our pathways however lack the self-similarity under scale transformations that a true fractal should exhibit, and thus we need to allow D_m to vary with r. In doing so we can no longer rigorously identify D_m with the dimension of the pathway cluster, but may loosely refer to it as the local dimensionality (as it may be regarded as the local contribution to the actual dimensionality of the object). The mass distribution function $M(r)$ is calculated as an average over several thousand randomly chosen center positions x_0 in the pathway (in order to obtain statistically independent results).

It is also useful to lend the concept of radial distribution functions commonly used in the analysis of diffraction data of amorphous materials. The reduced radial distribution function, $D(r)$, which we will use here, is defined as

$$D(r) = 4\pi r[\rho(r) - \rho_0], \tag{4}$$

where $\rho(r)$ is the pair correlation density and ρ_0 is the average number density of particles, or, in our case, the average cluster probability. The multiplicative factor of r in $D(r)$ amplifies small oscillations at larger radii that are difficult to discern by studying $\rho(r)$ directly, but one should be aware that this also tends to shift peaks towards slightly higher radii. By constructing a reduced radial distribution function for the cluster, where we calculate $\rho(r)$ over the volume elements in the cluster, instead of over atomic positions, we can directly compare correlations in the structure to correlations in the pathways.

4. Results

Fig. 2 shows a 4 Å thick slice through each of the salt doped glasses, depicting the conduction pathways. The

Table 1
The bond-valence parameters for the interaction between all mobile ions and anions present in the glasses in this study

	O^{2-}			I^-			Cl^-		
	R_0 (Å)	b (Å)	co (Å)	R_0 (Å)	b (Å)	co (Å)	R_0 (Å)	b (Å)	co (Å)
Ag^+	1.78239	0.394	5.0	2.08036	0.530	6.0	–	–	–
Li^+	1.1745	0.514	6.0	–	–	–	1.3873	0.640	6.0
Na^+	1.57658	0.475	6.0	–	–	–	1.6833	0.608	6.0

Included are also the cut-off radii (co), the largest distance over which a cat–anion pair can interact in the model.

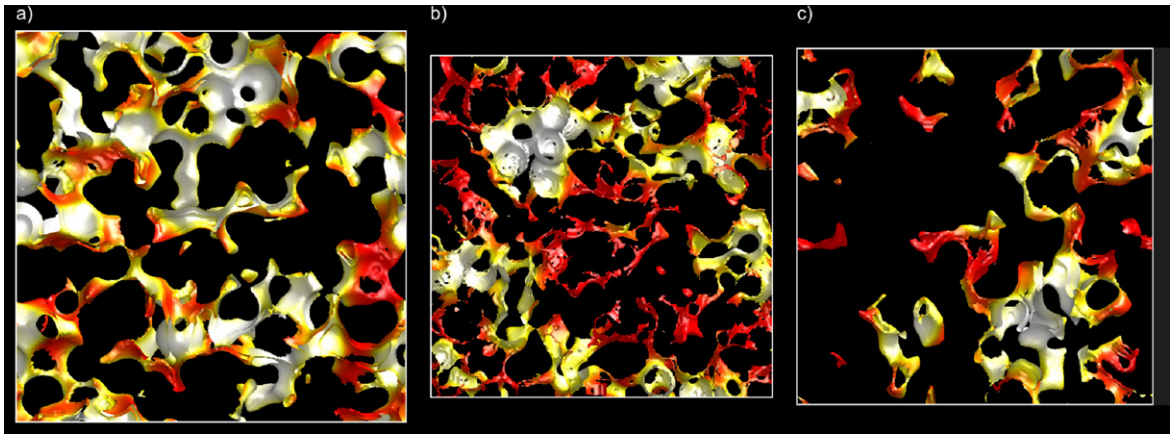

Fig. 2. 4 Å thick slices through the conduction pathways of (a) $(AgI)_{0.6}$–$(Ag_2O–2B_2O_3)_{0.4}$, (b) (LiCl)–$(Li_2O–2B_2O_3)$ and (c) (NaCl)–$(Na_2O–2B_2O_3)$. The color of the pathways reflects the local coordination of the mobile ions, with red parts being solely oxygen coordinated ions and white parts only halide coordinated ions. The three slices are depicted in scale to each other.

pathways have been colored according to the relative coordination to oxygen, with red[1] corresponding to a 100% oxygen coordinated part of the pathway and white parts having 100% halide coordination. Visual inspection already reveals some of the differences in structure between the three glasses. The conduction pathways of the AgI doped glass are well connected and homogenously distributed throughout the glass for the chosen threshold value Δ_0. Pathway regions resemble ribbons of sites that branch at typical distances of ca. 4 Å. Regions of mostly iodine-coordinated volume elements are connected by bridges of mostly oxygen coordinated. The LiCl doped glass differs in its pathway structure (for the same value of Δ_0) by being less homogenous than the pathways of the AgI doped glass. It is also more polarized in the relative coordination to oxygen/halide ions where salt-rich regions are connected by a network of oxygen coordinated pathways. They are considerably thinner than those parts of the pathway that have high chloride coordination. An even more inhomogeneous distribution of the pathways is found in the NaCl doped glass where large voids are clearly seen in the pathway structure. Although only one thin slice from each structure is shown here, they are relatively typical for each glass.

Using the concept of mass–radius dimension, we can further investigate details of the pathway structure. The derivative of the log–log plot of $M(r)$ vs. r, $D_m(r)$, for all glasses in this study is displayed in Fig. 3. We can identify four regions in these plots: (1) In the local region (up to ca. 2 Å), $D_m(r)$ is decreasing with increasing r and is dominated by the thickness of the pathways, i.e., a lower $D_m(r)$ means a thinner pathway. (2) After the minima in $D_m(r)$ we reach the branching region, where $D_m(r)$ increases and in some cases reaches values above 3. The sharper the increase, the better defined is the typical branching distance. (3) At length-scales above the first peak position follows a region where some of the glasses show small peaks due to an intermediate ordering of the pathways and finally (4) at sufficiently large r-values $D_m(r)$ approaches 3 as the structure

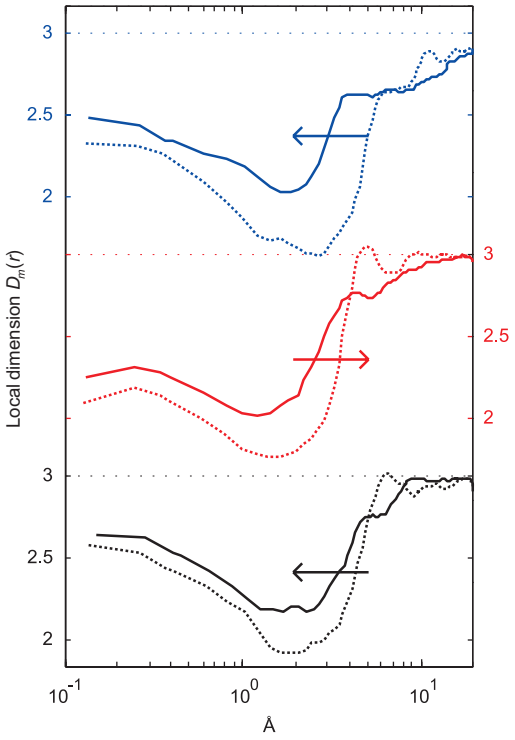

Fig. 3. The 'local dimension', $D_m(r)$ vs. r for all six glasses of this study, where the curves for the different mobile ions are shifted vertically for clarity. The Ag, Li and Na borates are shown in the bottom, middle and top, respectively. The salt doped glasses are marked by solid lines, whereas the undoped have dashed lines. Arrows indicate to which y-axis each curve belongs. Since many different structural models can be in quantitative agreement with the experimental diffraction data and the constraints applied in the RMC modeling, it is difficult to make a quantitative determination of the error bars. However, by comparing the results for different structure models of the same glass it is clear that the position of the features (which is discussed in this paper) have less than 10% errors, whereas the magnitude of $D_m(r)$ shows somewhat larger variations.

[1] For interpretation of the references in color, the reader is referred to the web version of this article.

within radius r becomes large enough to contain all statistically unique features of the pathway network. In the case of the salt doped glasses, the AgI doped has clearly the thickest pathways manifested by its high value of $D_m(r)$ at <2 Å. Otherwise region 2 is relatively similar for the doped glasses, whereas region 3 differs between them. The Ag pathways exhibit a sharp rise in $D_m(r)$ at 6–9 Å and the pathway reaches its limiting fractal dimension of three at length scales beyond 9 Å, whereas this region is less defined in the Li and Na pathways. For the NaCl doped glass the limit $D_m(r) = 3$ is not reached up to the maximum distance (half the side length of the structural model box, 17.8 Å in the NaCl doped borate glass), indicating that a somewhat larger structure model would be required to give a statistically complete description of the pathway structure. The pathways of the undoped glasses show a lower dimensionality in the local region but have a more well-defined branching region. This is an effect of having a single anion that creates a smaller spread in the typical branching distance. All the undoped glasses show also weak oscillations at multiples of the first peak due to an intermediate range ordering of the pathway network.

Reduced radial distribution functions, $D(r)$, of the pathway network in all the investigated glasses are shown in Fig. 4. $D(r)$ was averaged over 3600 volume elements in the percolating pathway. In the figure it is clear that all glasses exhibit a peak at distances <1 Å. This is a result of the competing linear r term and the $\rho(r) - \rho_0$ term which tends to 0 with increasing r. The amplitude of this peak correlates loosely to the thickness of the pathways. The doped glasses also share a clear peak at about 3.5–4.5 Å which can be attributed to correlations over the excluded volume around halide ions that are residing in the pathways.

The undoped Ag borate glass has two distinct peaks, one at 6.6 Å and a second weak at 11.2 Å. This indicates an intermediate range order of the pathways with a characteristic length scale of around 7 Å. When the dopant AgI salt is introduced into the glass we observe a halide peak at 4.5 Å and a second broader peak at 9.7 Å. Thus the dopant salt has increased the typical distance between neighboring parts of the pathway that are separated by boron–oxygen segments. These findings can be compared directly with results from neutron diffraction experiments [13]. Since the experimental $S(Q)$ is dominated by boron and oxygen correlations, the first sharp diffraction peaks (FSDP) at 1.3 $Å^{-1}$ in the undoped glass and 0.8 $Å^{-1}$ in the doped correspond to density fluctuations in the boron–oxygen network on length-scales of 4.8 and 8 Å, respectively. From these data and RMC modeling, the structure of both glasses have been asserted to consist of well defined borate chains separated by void channels in which the silver and (in the doped glass) iodine ions reside. Upon doping, these void channels expand and thus increase the characteristic correlation lengths. The present findings then suggest that the intermediate-range ordering in the pathway network is closely related to the density fluctuations in the boron–oxygen network.

The undoped Li and Na glasses both show some ordering of their pathways with peaks at 4.9 and 5.8 Å, respectively, followed by second peaks at roughly twice these lengths (9.7 and 11.1 Å). These values correspond fairly well to structural correlation lengths obtained by neutron diffraction [14]. The density fluctuations in the boron–oxygen network were found to have characteristic lengths of 4.1 Å in the Li borate glass and 4.7 Å in the Na borate glass. Upon doping this order is lost in both glasses and the only remaining structure of $D(r)$ is the halide peak. While $D(r)$ of the Li pathways drops quickly and only fluctuates around zero for $r > 6$ Å, the Na glass exhibits a clear tendency of clustering of the pathways. This disorder in the pathway network is expected since it reflects the inhomogeneous distribution of the salt ions. Thus in these two glasses the voids in the boron–oxygen network are, in contrast to those in the AgI doped glass, of widely different sizes and shapes [14].

5. Discussion

Though substantial efforts to understand the conduction mechanism in glasses have been made, we are still lacking a

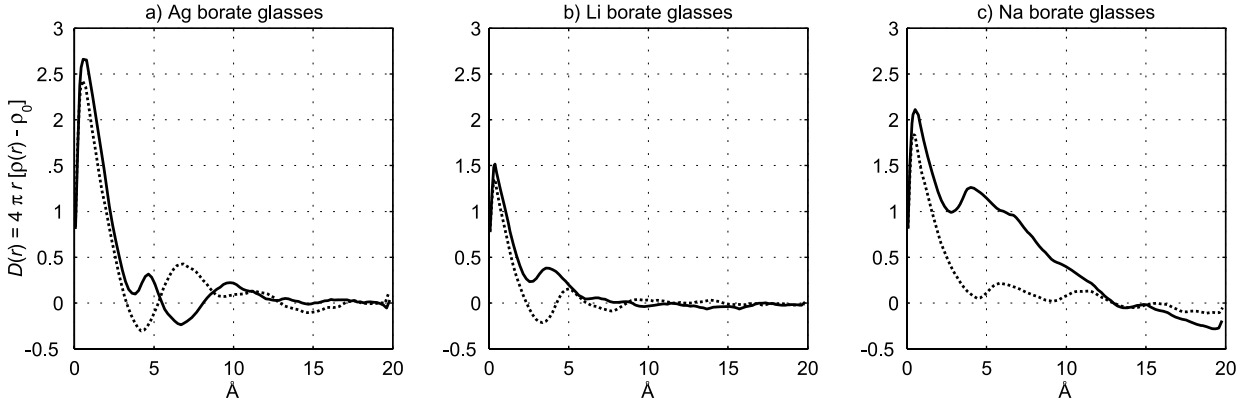

Fig. 4. Reduced radial distribution function of the pathway network in (a) $(AgI)_x$–$(Ag_2O–2B_2O_3)_{1-x}$, (b) $(LiCl)_x$–$(Li_2O–2B_2O_3)_{1-x}$ and (c) $(NaCl)_x$–$(Na_2O–2B_2O_3)_{1-x}$. Solid lines are used for the doped glasses whereas the undoped are plotted as dashed lines. The error analysis discussed in Fig. 3 is valid also for these data. Thus, the error of the correlation length discussed in the text should be less than 10%.

generally accepted theory that can account for their ionic properties. In the case of $(AgI)_x-(Ag_2O-2B_2O_3)_{1-x}$ it has been suggested that its high conductivity, at least to some extent, is due to the high intermediate range ordering of the borate chains and the void channels in which the ion transport have been assumed to occur. The dopant salt is homogenously distributed in the glass matrix and expands the void channels, creating a characteristic length of 8 Å in the borate network. Thus, the previously observed [13] expansion of the borate network is directly related to the expansion of the conduction pathways observed in this study. Turning to the LiCl and NaCl doped borate glasses we see that the salt ions have an inhomogeneous distribution in these glasses, which drastically reduces the intermediate range order of both the glass matrix and the conduction pathways. The increase in ionic conductivity upon salt doping is of the same order for the three glass systems. This investigation thus renders it improbable that the particular intermediate range order in the AgI doped borate glass has a major effect on the conductivity. This is not an unexpected finding considering that we have earlier found [24] a correlation between the ionic conductivity and the volume fraction of the percolating pathway, a property that is highly dependent on the softness of the bonds made by the mobile ion. Thus, although it is important for the conductivity that the pathways are wide and form an extended and percolating network, this study does not indicate that an ordering of the pathway network or the glass structure enhances the conductivity. This issue will be further elucidated by making comparable calculations for more or less randomly generated glass structures.

6. Conclusions

This work has shown that the conduction pathways in borate glasses exhibit a similar change in ordering upon salt doping as the glass network itself. While the Ag borates have an intermediate order in both atomic structure and conduction pathways, the NaCl and LiCl doped glasses both lose the ordering that exists in the corresponding undoped glasses. Given that all glasses show a similar increase in conductivity upon salt doping, we may conclude that the particular ordering of the AgI doped glass is not an important factor for its high conductivity.

Acknowledgment

This work was financially supported by the Swedish Foundation for Strategic Research which is gratefully acknowledged.

References

[1] M.D. Ingram, Phys. Chem. Glasses 28 (1987) 215.
[2] R.L. McGreevy, L. Pusztai, Mol Simul. 1 (1988) 359.
[3] D.A. Keen, R.L. McGreevy, Nature 344 (1990) 423.
[4] K. Falconer, Fractal Geometry, Wiley, 2003.
[5] C. Chiodelli, A. Magistris, M. Villa, J.L. Bjorkstam, J. Non-Cryst. Solids 51 (1982) 143.
[6] G.E. Jellison Jr., S.A. Feller, P.J. Bray, Phys. Chem. Glasses 19 (1978) 52.
[7] Y.H. Yun, P.J. Bray, J. Non-Cryst. Solids 27 (1978) 363.
[8] S.A. Feller, W.J. Dell, P.J. Bray, J. Non-Cryst. Solids 51 (1982) 21.
[9] F. Galeener, G. Lucovsky, J.C. Mikkelsen Jr., Phys. Rev. B 22 (1980) 3983.
[10] J. Lorösch, M. Couzi, J. Pelous, R. Vacher, A. Levasseur, J. Non-Cryst. Solids 69 (1984) 1.
[11] E.I. Kamitsos, A.P. Patsis, M.A. Karakassides, G.D. Chryssikos, J. Non-Cryst. Solids 126 (1990) 52.
[12] J. Swenson, L. Börjesson, W.S. Howells, Phys. Rev. B 52 (1995) 9310.
[13] J. Swenson, L. Börjesson, R.L. McGreevy, W.S. Howells, Phys. Rev. B 55 (1997) 11236.
[14] J. Swenson, L. Börjesson, W.S. Howells, Phys. Rev. B 57 (1998) 13514.
[15] G. Carini, M. Cutroni, A. Fontana, G. Mariotto, F. Rocca, Phys. Rev. B 29 (1984) 3567.
[16] St. Adams, J. Swenson, Phys. Rev. B 63 (2000) 054201.
[17] J. Swenson, St. Adams, Ionics 9 (2003) 28.
[18] H.L. Tuller, D.P. Button, in: F.W. Poulsen, N. Hessel-Andersen, K. Clausen, S. Skaarup, O. Soerensen (Eds.), Transport–Structure Relations in Fast Ion and Mixed Conductors, Risø National Laboratory, Roskilde, Denmark, 1985, p. 119.
[19] G. Chiodelli, G. Campari Vigano, G. Flor, A. Magistris, M. Villa, Solid State Ion. 8 (1983) 311.
[20] St. Adams, J. Swenson, J. Phys.: Condens. Matter 17 (2005) S87.
[21] I.D. Brown, The Chemical Bond in Inorganic Chemistry – The Bond Valence Model, Oxford University, 2002.
[22] St. Adams, Acta Crystallogr. Sect. B: Struct. Sci. B 57 (2001) 278.
[23] A. Hall, St. Adams, J. Swenson, Phys. Rev. B, in press.
[24] St. Adams, J. Swenson, Phys. Rev. Lett. 84 (2000) 4144.